Magnetoelastic Effects in Iron Telluride

I. Paul[1], A. Cano[2] and K. Sengupta[3]
[1] *Institut Néel, CNRS/UJF, 25 avenue des Martyrs, BP 166, 38042 Grenoble, France.*
[2] *European Synchrotron Radiation Facility, 6 rue Jules Horowitz, BP 220, 38043 Grenoble, France.*
[3] *Theoretical Physics Department, Indian Association for the Cultivation of Science, Kolkata-700032, India.*
(Dated: November 10, 2010)

Iron telluride doped lightly with selenium is known to undergo a first order magneto-structural transition before turning superconducting at higher doping. We study the effects of magneto-elastic couplings on this transition using symmetry considerations. We find that the magnetic order parameters are coupled to the uniform monoclinic strain of the unit cell with one iron per cell, as well as to the phonons at high symmetry points of the Brillouin zone. In the magnetic phase the former gives rise to monoclinic distortion while the latter induces dimerization of the ferromagnetic iron chains due to alternate lengthening and shortening of the nearest-neighbour iron-iron bonds. We compare this system with the iron arsenides and propose a microscopic magneto-elastic Hamiltonian which is relevant for all the iron based superconductors.

PACS numbers: 74.70.Xa, 74.90.+n, 75.80.+q

I. INTRODUCTION

Selenium-doped iron telluride, $FeTe_{1-x}Se_x$, is one of the several classes of iron based materials which are currently being studied for their intriguing superconducting properties.[1–5] This material, the so-called 11 system, exhibits a magneto-structural transition at low carrier doping that is suppressed by the emergence of superconductivity at large enough doping (or under applied pressure).[6] This feature of the phase diagram is shared by the rest of iron-based superconductors,[7] namely the 1111 systems with chemical composition *Re*OFeAs where *Re* refers to a rare earth metal (e.g., La, Ce and Sm),[8] the 111 systems with composition *A*FeAs where *A* refers to an alkali metal (e.g., Na and Li),[9] and the 122 systems composed of $AeFe_2As_2$ where *Ae* is an alkali earth metal (e.g., Ba, Sr and Ca).[10] LiFeAs is the only exception to this rule, as the parent compound is already a superconductor.[11] In Ref. 12 a general phase diagram for the 1111, 122 and 111 systems was proposed on the basis of symmetry considerations which explained the salient features of the magnetic and structural transitions. The key ingredient for this general phase diagram is the magneto-elastic coupling between the magnetic and the structural order parameters. In this paper we show that similar symmetry-allowed couplings are also present in the 11 material, and are important in the sense that they give rise to experimentally observable structural distortions in the magnetic phase. Our description is based on a Ginzburg-Landau mean field analysis of the magneto-structural transition of iron telluride followed by a comparison with the iron arsenide systems. Furthermore, we propose a microscopic hamiltonian that provides a unified description of the magneto-elastic properties of all the iron-based superconductors.

Selenium doped iron telluride is represented as $Fe_{1+y}Te_{1-x}Se_x$ due to the presence of excess Fe in the interstitial positions of the Te layer.[13] The amount of excess Fe decreases with increasing selenium doping, and the phase diagram of the undoped compound is known to depend upon the amount of excess Fe.[4] In the following we focus on the system with $y \approx 0.076$ in the undoped state ($x = 0$). It is known to undergo a first-order transition at around 65 K from a high temperature paramagnetic tetragonal phase to a low temperature antiferromagnetic monoclinic phase (throughout the paper we follow the notations of an unit cell with 1Fe/cell).[14] The transition temperature decreases with increasing x, but the structural distortion remains concomitant with the magnetic transition. This makes the 11 material different from the 1111 and 111 systems, where there are two separate transitions at all doping, and also from the 122 system where the single transition splits into two transitions with doping. More importantly, the symmetry breaking associated with the magneto-structural transition of the telluride system is different from that of the arsenides. Thus, the low-temperature phase of the 11 system (Fig. 1) is monoclinic and is a bicollinear antiferromagnet with wavevector $(\pi/2, \pi/2)$ in the ab plane,[14–16] in contrast to the low-temperature phase of the iron arsenides (Fig. 2) which is orthorhombic and is a collinear antiferromagnet with wavevector $(\pi, 0)$. However, despite these apparent differences, in the following we show that a feature common to all the iron based superconductors is the presence of important magneto-elastic couplings whose microscopic origins appear to be the same.

The magneto-structural transition of $Fe_{1+y}Te_{1-x}Se_x$ has been studied earlier from a field theoretic point of view without taking into account all possible magneto-elastic terms.[17] At a more microscopic level the $(\pi/2, \pi/2)$ magnetic structure is somewhat puzzling from a weakly correlated band picture because, unlike the case of the iron arsenide materials, the magnetic ordering does not correspond to a nesting wavevector of the Fermi surface sheets. This has motivated theorists to seek rationale in models that are based on strong correlation physics such as a localized spin model[18] or that describing magnetism induced by orbital ordering.[19] Alternately, it has

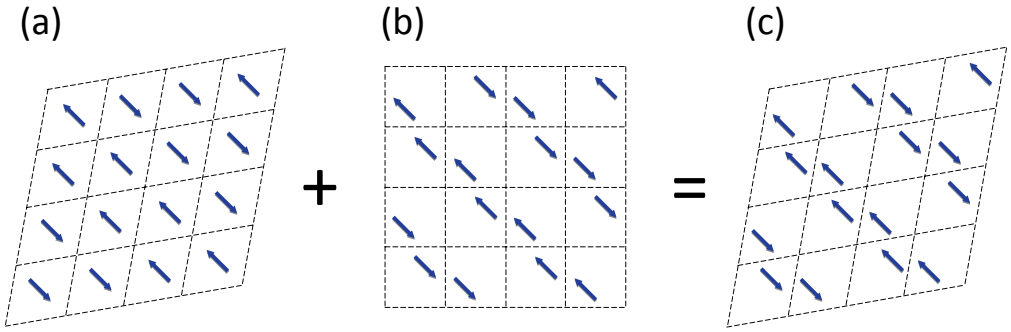

FIG. 1: Low temperature magneto-structural pattern on the ab plane formed by the Fe atoms of $Fe_{1+y}Te_{1-x}Se_x$. The spins order with wavevector $(\pi/2, \pi, 2)$ forming a bicollinear antiferromagnet. The associated structural change (c) is a combination of a monoclinic distortion (a) of the square lattice, and a dimerization (b) of the ferromagnetic Fe chains due to alternate lengthening and shortening of the nearest-neighbour Fe-Fe bonds.

also been argued that doping due to excess Fe changes the Fermi surface sufficiently such that $(\pi/2, \pi/2)$ is indeed a nesting wavevector.[20]

The rest of the paper is organized as follows. In the next section we describe the magneto-structural transition by a Ginzburg-Landau free energy whose form is independent of the microscopic details. The $(\pi/2, \pi/2)$ magnetic structure is described by four $O(3)$ magnetic order parameters which gives rise to several symmetry allowed magneto-elastic couplings. Thus, the magnetic order parameters are coupled to the monoclinic component of the uniform strain, as well as to the lattice distortions associated with wavevectors of high symmetry in the Brillouin zone. In the magnetic phase the former coupling distorts the lattice monoclinically with long and short next-nearest-neighbour Fe-Fe bonds (Fig. 1a), while the latter produces long and short nearest-neighbour Fe-Fe bonds which gives rise to dimerization of the ferromagnetic chains (Fig. 1b). The experimental observation of both these distortions indicate that the magneto-elastic terms are non-negligible.[14–16] Furthermore, we find that the effective magnetic free energy generated by the lattice favours a first order transition, as observed experimentally. We finish section II by briefly recalling the mean field description of the iron arsenides, and by comparing it with the iron telluride system. In section III we propose a microscopic hamiltonian which compactly describes the magneto-elastic properties of all the iron based superconductors, and we conclude in section IV by pointing out directions for future research.

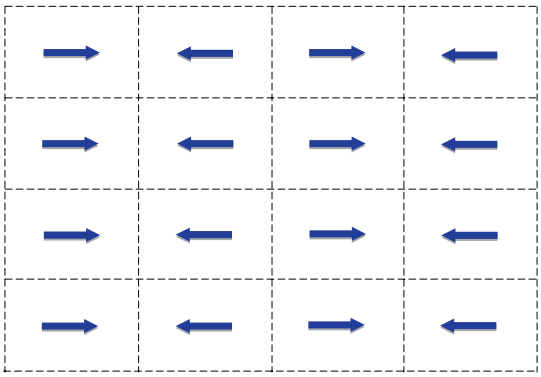

FIG. 2: Low temperature magneto-structural pattern on the ab plane formed by the Fe atoms of the iron arsenide systems. The spins order with wavevector $(\pi, 0)$ forming a collinear antiferromagnet. The associated structural change is an orthorhombic distortion of the square lattice.

II. GINZBURG-LANDAU THEORY

A. Iron telluride

The Ginzburg-Landau free energy describing the phase transition can be expressed as

$$F_{GL} = F_M + F_E + F_{ME} \tag{1}$$

corresponding to the magnetic, elastic and the magneto-elastic parts respectively. Hereafter the notation refers to the ab plane of the system where the symmetry considerations are non-trivial.

The magnetic sector is described by four $O(3)$ order parameters which are the Fourier components $\mathbf{M}_i$ with $i = 1, \ldots, 4$, of the magnetization ($\mathbf{M}$) corresponding to the wavevectors $\mathbf{q}_1 = (\pi/2, \pi/2) = -\mathbf{q}_3$, and $\mathbf{q}_2 = (-\pi/2, \pi/2) = -\mathbf{q}_4$. Thus, at the mean field level the magnetization is given by $\mathbf{M}(\mathbf{r}_n) = \sum_{i=1}^{4} \mathbf{M}_i \exp(i\mathbf{q}_i \cdot \mathbf{r}_n)$, where $\mathbf{r}_n$ denotes a lattice position. Since $\mathbf{M}(\mathbf{r}_n)$ is real, we have $\mathbf{M}_1 = \mathbf{M}_3^*$ and $\mathbf{M}_2 = \mathbf{M}_4^*$. Alternatively, one can define four real-valued $O(3)$ order parameters $\mathbf{L}_i$ with $i = 1, \ldots, 4$, such that $\mathbf{M}_1 = [(\mathbf{L}_1 + \mathbf{L}_3) - i(\mathbf{L}_1 - \mathbf{L}_3)]/2$ and $\mathbf{M}_2 = [(\mathbf{L}_2 + \mathbf{L}_4) - i(\mathbf{L}_2 - \mathbf{L}_4)]/2$. In terms of $\mathbf{L}_i$ the magnetization is

$$\mathbf{M}(\mathbf{r}_n) = \sum_{i=1}^{4} \mathbf{L}_i \left[\cos(\mathbf{q}_i \cdot \mathbf{r}_n) + \sin(\mathbf{q}_i \cdot \mathbf{r}_n)\right].$$

The lattice sector is described by means of the strain tensor ϵ_{ij} which can be written as $\epsilon_{ij}(\mathbf{r}_n) = u_{ij} + \frac{i}{2}\sum_{\mathbf{q}\neq 0}[q_i u_j(\mathbf{q}) + q_j u_i(\mathbf{q})]e^{i\mathbf{q}\cdot\mathbf{r}_n}$. Here u_{ij} describes uniform strains and $\mathbf{u}(\mathbf{q})$ is the Fourier transform of the displacement field $\mathbf{u}(\mathbf{r}_n)$.[21] At the mean field level and to the lowest order in an expansion of the free energy in terms of the order parameters, we find that the elastic variables that couple with the magnetic ones are the shear component u_{xy} and the quantities $\mathbf{u}_i \equiv \mathbf{u}(\mathbf{q}_i)$ with $i = 5, 6$ and 7 corresponding to $\mathbf{q}_5 = (\pi, \pi)$, $\mathbf{q}_6 = (\pi, 0)$ and $\mathbf{q}_7 = (0, \pi)$.

The transformation of the above variables under the symmetry operations of the square lattice are summarized in Table I, using which one can construct F_{GL} from the terms that are allowed by symmetry. In the following we assume $O(3)$ symmetry in the magnetic sector, which amounts to neglecting spin-orbit coupling. The magnetic part of the free energy can be expressed as

$$F_M = \frac{A}{2}\left(\mathbf{L}_1^2 + \mathbf{L}_2^2 + \mathbf{L}_3^2 + \mathbf{L}_4^2\right) + \ldots, \tag{2}$$

where $A = A'(T - T_N)$ is the only temperature (T) dependent coefficient, and T_N is temperature for the magneto-structural transition. The ellipses denote the fourth order and the sixth order terms, the latter being necessary because eventually the transition is first order. At the fourth order there are seven invariant terms namely, (i) $\sum_i L_i^4$, (ii) $L_1^2 L_2^2$ + cyclic terms, (iii) $(\mathbf{L}_1 \cdot \mathbf{L}_2)^2$ + cyclic terms, (iv) $(\mathbf{L}_1 \cdot \mathbf{L}_3)(\mathbf{L}_2 \cdot \mathbf{L}_4)$, (v) $(\mathbf{L}_1 \cdot \mathbf{L}_2)(\mathbf{L}_3 \cdot \mathbf{L}_4) + 2 \leftrightarrow 4$, (vi) $(\mathbf{L}_1 \cdot \mathbf{L}_3)^2 + (\mathbf{L}_2 \cdot \mathbf{L}_4)^2$, and (vii) $L_1^2 L_3^2 + L_2^2 L_4^2$. Thus, at this order there are seven independent coupling constants in terms of which the phase diagram described by F_M is rather rich. It is not the purpose of this paper to investigate how the phase diagram varies with different couplings, which is anyway a formidable task. The experimentally observed magnetic state is described by a non-zero value of any one of the $\mathbf{L}_i$, and the energetics of this choice is clearly beyond symmetry based arguments and mean field theory. Consequently, we do not write explicitly the terms beyond quadratic order. Next, the elastic part of the free energy is given by

$$F_E = \frac{c_{66}}{2}u_{xy}^2 + \frac{\Omega_1}{2}\mathbf{u}_5^2 + \frac{\Omega_2}{2}\left(\mathbf{u}_6^2 + \mathbf{u}_7^2\right), \tag{3}$$

where c_{66} is the elastic constant for monoclinic distortion, and Ω_1 and Ω_2 are the elastic stiffness of the displacements at the respective wavevectors. Since the elastic sector is not critical, it is sufficient to truncate the expansion at the quadratic order. Finally, using Table I, the lowest order magneto-elastic part is given by

$$\begin{aligned} F_{ME} &= g_1 u_{xy}\left(L_1^2 + L_3^2 - L_2^2 - L_4^2\right) \\ &+ g_2\left[u_5^x\left(L_1^2 - L_3^2 - L_2^2 + L_4^2\right) + u_5^y\left(L_1^2 - L_3^2 + L_2^2 - L_4^2\right)\right] \\ &+ g_3\left[u_6^x\left(\mathbf{L}_1 \cdot \mathbf{L}_4 - \mathbf{L}_2 \cdot \mathbf{L}_3\right) + u_7^y\left(\mathbf{L}_1 \cdot \mathbf{L}_2 - \mathbf{L}_3 \cdot \mathbf{L}_4\right)\right]. \end{aligned} \tag{4}$$

In the above we ignore the standard magneto-striction term since it is present in all materials, and is not peculiar to the 11 system.

We minimize F_{GL} with respect to the elastic degrees of freedom and we get

$$u_{xy} = -\frac{g_1}{c_{66}}\left(L_1^2 + L_3^2 - L_2^2 - L_4^2\right), \tag{5a}$$

$$u_5^{x/y} = -\frac{g_2}{\Omega_1}\left(L_1^2 - L_3^2 \mp L_2^2 \pm L_4^2\right), \tag{5b}$$

$$u_6^x = -\frac{g_3}{\Omega_2}\left(\mathbf{L}_1 \cdot \mathbf{L}_4 - \mathbf{L}_2 \cdot \mathbf{L}_3\right), \tag{5c}$$

$$u_7^y = -\frac{g_3}{\Omega_2}\left(\mathbf{L}_1 \cdot \mathbf{L}_2 - \mathbf{L}_3 \cdot \mathbf{L}_4\right), \tag{5d}$$

while the remaining elastic variables are zero at equilibrium. Thus, the lattice mediated effective magnetic free energy is given by

$$\begin{aligned} F'_M &= (F_E + F_{ME})_{\text{equilib}} \\ &= -\frac{g_1^2}{2c_{66}}\left(L_1^2 + L_3^2 - L_2^2 - L_4^2\right)^2 \\ &- \frac{g_2^2}{2\Omega_1}\left[\left(L_1^2 - L_3^2 - L_2^2 + L_4^2\right)^2 + \left(L_1^2 - L_3^2 + L_2^2 - L_4^2\right)^2\right] \\ &- \frac{g_3^2}{2\Omega_2}\left[\left(\mathbf{L}_1 \cdot \mathbf{L}_4 - \mathbf{L}_2 \cdot \mathbf{L}_3\right)^2 + \left(\mathbf{L}_1 \cdot \mathbf{L}_2 - \mathbf{L}_3 \cdot \mathbf{L}_4\right)^2\right]. \end{aligned} \tag{6}$$

The simple exercise above allows us to make the following two points about the experimentally observed magnetic phase where $L_1 = L$ (say) is the spontaneous magnetization and the remaining L_i are zero. (i) The lattice undergoes a monoclinic distortion with $u_{xy} = -g_1 L^2/c_{66}$ producing long and short next-nearest-neighbour Fe-Fe bonds (Fig. 1a). Simultaneously, the nearest-neighbour Fe-Fe bonds dimerize such that $u_5^x = u_5^y = -g_2 L^2/\Omega_1$ (Fig. 1b). The experimental observation of both these distortions imply that the magneto-elastic coupling is non-negligible.[14,16] (ii) The lattice mediated effective magnetic free energy is given by $F'_M = -(g_1^2/c_{66} + g_2^2/\Omega_1)L^4/2$, which is a negative contribution to the free energy at fourth order. As such, this contribution favours the experimentally observed first order transition.

B. Iron arsenides

To finish this section we briefly recall the magneto-elastic properties of the iron arsenides (Fig. 2), studied in detail in Ref. 12, in order to compare them with the 11 material and to facilitate the discussion in the following section. The relevant magnetic order parameters for the iron arsenides are the Fourier components $\mathbf{M}_6$ and $\mathbf{M}_7$ of the magnetization corresponding to the wavevectors $\mathbf{q}_6$ and $\mathbf{q}_7$ respectively. They couple to the orthorhombic component $u_{xx} - u_{yy}$ of the uniform strain tensor, and at the mean field level the magneto-elastic part has the form[22]

$$F_{ME}^{\text{FeAs}} = g_4\left(u_{xx} - u_{yy}\right)\left(M_6^2 - M_7^2\right). \tag{7}$$

		reflections		translations	
	90° rotation	x-axis	$x=y$ axis	along x	along y
$\mathbf{L}_1$	$\mathbf{L}_2$	$\mathbf{L}_4$	$\mathbf{L}_1$	$\mathbf{L}_3$	$\mathbf{L}_3$
$\mathbf{L}_2$	$\mathbf{L}_3$	$\mathbf{L}_3$	$\mathbf{L}_4$	$-\mathbf{L}_4$	$\mathbf{L}_4$
$\mathbf{L}_3$	$\mathbf{L}_4$	$\mathbf{L}_2$	$\mathbf{L}_3$	$-\mathbf{L}_1$	$-\mathbf{L}_1$
$\mathbf{L}_4$	$\mathbf{L}_1$	$\mathbf{L}_1$	$\mathbf{L}_2$	$\mathbf{L}_2$	$-\mathbf{L}_2$
u_{xy}	$-u_{xy}$	$-u_{xy}$	u_{xy}	u_{xy}	u_{xy}
(u_5^x, u_5^y)	$(u_5^y, -u_5^x)$	$(u_5^x, -u_5^y)$	(u_5^y, u_5^x)	$(-u_5^x, -u_5^y)$	$(-u_5^x, -u_5^y)$
(u_6^x, u_6^y)	$(u_7^y, -u_7^x)$	$(u_6^x, -u_6^y)$	(u_7^y, u_7^x)	$(-u_6^x, -u_6^y)$	(u_6^x, u_6^y)
(u_7^x, u_7^y)	$(u_6^y, -u_6^x)$	$(u_7^x, -u_7^y)$	(u_6^y, u_6^x)	(u_7^x, u_7^y)	$(-u_7^x, -u_7^y)$

TABLE I: Transformation properties of the magnetic and the elastic order parameters under symmetry operations of the square lattice. The definitions of the various order parameters are given following Eq. (1).

This term determine (a) if there is a single magneto-structural transition (as in the undoped 122 systems) or two separate transitions (as in the 1111 or the sufficiently doped 122 systems), (b) the order (first versus second) of the transitions, and (c) why the system prefers a collinear magnetic state instead of a non-collinear order.

In the case of the iron arsenides, since the system is near an orthorhombic transition (this is explicit in the phase diagram of the 1111 and the doped 122 systems) where the corresponding elastic constant c_o vanishes, it is possible to argue that the energy scale $g_4^2/|c_o|$ generated magneto-elastically is dominant and controls the main features of the phase diagram for the magneto-structural transition. In contrast, the phase diagram of the 11 system does not exhibit a monoclinic structural transition where c_{66} vanishes, and since the magnitude of c_{66} from ultrasound experiments is currently unavailable to us, a similar argument for the scale $g_1^2/|c_{66}|$ cannot be made at present. Nevertheless, the distortions of the lattice of the undoped 122 systems and the 11 systems on entering the magnetic phase provide clear evidence that the magneto-elastic terms are non-negligible and ubiquitous for all the iron based superconductors.

III. MICROSCOPIC COUPLING

In the previous section we argued in favour of the existence of magneto-elastic couplings in all the iron based superconductors. The precise form of the couplings at the mean field level differs between the iron arsenides and the 11 systems because the magnetic order parameters in these two classes are different. In the following we introduce a microscopic magneto-elastic hamiltonian whose mean field form captures both Eqs. (4) and (7). The purpose of such a hamiltonian is two-fold. Firstly, to unify the various magneto-elastic effects observed in different classes of systems and provide a common description. This is a first step to understand the microscopic origin of these couplings. Secondly, to go beyond mean field theory and study the effect of these couplings at the level of fluctuations.

The simplest microscopic magneto-elastic hamiltonian is given by

$$\mathcal{H}_{ME} = \sum_{n,\delta} \lambda_\delta \left(\mathbf{S}_{n+\delta} \cdot \mathbf{S}_n\right) \mathbf{r}_{n,\delta} \cdot \left[\mathbf{u}(\mathbf{r}_{n+\delta}) - \mathbf{u}(\mathbf{r}_n)\right], \quad (8)$$

where n denotes lattice sites, δ implies nearest-neighbours and next-nearest-neighbours, $\mathbf{r}_{n,\delta} = \mathbf{r}_{n+\delta} - \mathbf{r}_n$, λ_δ is the strength of the coupling that can depend on the bond lengths and the bond angles, and $\mathbf{S}_n$ is the electron spin at site n. It is easy to verify that when the spins $\mathbf{S}_n$ and the displacements $\mathbf{u}(\mathbf{r}_n)$ are replaced by the appropriate mean field variables, one obtains the mean field results of Eqs. (4) and (7). Thus, while the coupling $g_1 = -4\lambda_{nnn}$ originates from the next-nearest-neighbour magneto-elastic interaction λ_{nnn}; g_2, g_3 and g_4 are obtained from nearest-neighbour interaction λ_{nn}, implying that in the 11 system, in fact, $g_2 = g_3 = -4\lambda_{nn}$. Experimentally, all the different kinds of distortions in the 1111, the 122 and the 11 systems that have been reported are such that the ferromagnetic bonds are shorter than the corresponding antiferromagnetic bonds,[14,16,23,24] which implies that $\lambda_\delta > 0$. Hamiltonians of the above type are quite common in the study of lattice effects in insulating magnetic systems, where $\lambda_\delta \propto \partial J/\partial r$ is the variation of the Heisenberg exchange coupling J with distance. Consequently, it is likely that the magneto-elastic effects are manifestations of strong coupling physics. Indeed many authors have argued that the magnetic properties of these systems are more suitably described by localized spin models rather than a weak coupling band picture.[25]

IV. SUMMARY

To summarize, in this paper we studied the effects of magneto-elastic couplings on the magnetic phase transition in $Fe_{1+y}Te_{1-x}Se_x$. From symmetry considerations we showed that on entering the magnetic phase, these couplings give rise to uniform monoclinic distortion (Fig. 1a) of the unit cell with one Fe/cell, and also induce dimerization (Fig. 1b) of the ferromagnetic Fe chains due

to alternate lengthening and shortening of the nearest-neighbour Fe-Fe bonds. We also showed that the effective magnetic energy generated by the lattice favours a first order transition. Finally, we compared this system with the iron arsenide systems, and we proposed a microscopic hamiltonian to describe the magneto-elastic effects in both these classes of iron based superconductors. In the future we hope to study the effect of these couplings on the magnetism and the superconductivity.

Acknowledgments

We are very thankful to W. Bao, O. Cepas, M. Civelli A. Martinelli, A. Vishwanath, and T. Ziman for insightful discussions. I.P. is thankful for the hospitality of the Indian Association for the Cultivation of Sciences where this work was initiated. K.S. thanks DST, India for support through project no. SR/S2/CMP-001/2009.

[1] F.-C. Hsu *et. al.*, Proc. Natl. Acad. Sci. U.S.A, **105** 14262 (2008).
[2] K.-W. Yeh *et. al.*, Europhys. Lett. **84** 37002 (2008).
[3] See e.g., B. C. Sales *et. al.*, Phys. Rev. B **79** 094521 (2009).
[4] For a review see, e.g., Y. Mizuguchi, and Y. Takano, J. Phys. Soc. Jpn. **79**, 102001 (2010).
[5] T. Klein *et. al.*, arXiv:10100493.
[6] G. Garbarino *et. al.*, Europhys. Lett. **86**, 27001 (2009).
[7] For reviews see e.g., M. Norman, Physics **1**, 21 (2008); D. C. Johnston, arXiv:1005.4392.
[8] Y. Kamihara *et. al.*, J. Am. Chem. Soc. **130**, 3296 (2008).
[9] S. Li *et. al.*, Phys. Rev. B **80**, 020504(R) (2009).
[10] See e.g., M. Rotter, M. Tegel, and D. Johrendt, Phys. Rev. Lett. **101**, 107006 (2008).
[11] See e.g., J. H. Tapp *et. al.*, Phys. Rev. B **78**, 060505(R) (2008).
[12] A. Cano *et. al.*, Phys. Rev. B **82**, 020408(R) (2010).
[13] F. Gronvold, H. Haraldsen, and J. Vihovde, Acta Chem. Scand. 8, 1927 (1954).
[14] W. Bao *et. al.*, Phys. Rev. Lett. **102**, 247001 (2009).
[15] S. Li *et. al.*, Phys. Rev. B **79**, 054503 (2009).
[16] A. Martinelli *et. al.*, Phys. Rev. B **81**, 094115 (2010).
[17] C. Xu and J. Hu, arXiv:0903.4477.
[18] C. Fang, B. A. Bernevig, and J. Hu, Europhys. Lett. **86**, 67005 (2009).
[19] A. M. Turner, F. Wang, and A. Vishwanath, Phys. Rev. B **80**, 224504 (2009).
[20] M. J. Han and S. Y. Savrasov, Phys. Rev. Lett. **103**, 067001 (2009).
[21] A. I. Larkin and S. A. Pikin, Zh. Eksp. Teor. Fiz. **56**, 1664 (1969) [Sov. Phys. JETP **29**, 891 (1969)].
[22] Here the notations are different from Ref. 12 because the latter adopted the convention for a unit cell with two Fe/cell. Expressed in the notations of this paper the magnetic order parameters in Ref. 12 are $\mathbf{L}_{1/2} = \mathbf{M}_6 \pm \mathbf{M}_7$, and the monoclinic distortion in Ref. 12 is equivalent to an orthorhombic distortion when the principal axes are rotated 45°.
[23] See, e.g., C. de la Cruz et al., Nature (London) **453**, 899 (2008).
[24] A. Martinelli (private communication); W. Bao (private communication).
[25] See, e.g., Q. Si and E. Abrahams, Phys. Rev. Lett. **101**, 076401 (2008).